ISSN 2706-655X Vol.5, Issue 8: 42-48, DOI: 10.25236/IJFET.2023.050807

A Research of the Springback Effect Based on U-Shaped Deformation

Zikai Zhao, Xiaobing Bu, Qingxiang Guo, Yanting Zheng, Wenxiao Tan

China Automotive Technology & Research Center Co. Ltd, Tianjin, China

Abstract: *Steel-stamping is widely used in manufacturing metal parts procedures. However, a distinct spring-back effect happens on the metals after unloading. Such change may go against the original intention of the designers. Therefore, the study of the spring-back development after deep-drawing procedures is essential. In this report, the Nonlinear Finite Element Analysis is performed to predict the unloaded topology of a specific metal sheet. Besides, simulation results based on shell elements and 3D elements are compared.*

Keywords: *Steel-stamping, Spring-back effect, Nonlinear Finite Element Analysis*

1. Introduction

The elastically driven change of a metal sheet topology during unloading is Spring-back. It is essential to predict the final geometry of the part after spring-back before the manufacturing process. However, the process of gaining the ideal shape of the metal sheet is an expensive operation, considering the shape-modification of the punch and die. As a result, an economic method to operate the trial-and-error process is inevitable.

Nowadays, numerical methods had been proved acceptable to predict the material behaviour in sheet metal spring-back effect. [1,2,3] Though numerical analysis of an industrial design is less accurate than the experiment, more details of the deformed steel sheet, such as the stress gradient inside the twisted part, can expose through numerical analysis.

Setting the mathematical models of material properties is essential for studying the spring-back properties of sheet metals. Nonetheless, this paper will only consider the ideal element for predicting the spring-back effect. So, balancing the computational time and the accuracy of the simulation, the isotropic hardening model is applied. [4]

Since the sheet-like geometry of the blank part, choosing both shell elements and 3-D elements are reasonable for the prediction of the spring effect. The following discussion will introduce the available element type and discuss the element chosen for the simulation.

The incompatible element introduces additional degrees of freedom to enhance the element deformation gradient into the linear element. Furthermore, the element avoids overlapping or fissure of displacement fields at the boundary of elements. As a result, the incompatible mode linear element could behave as accurately as quadratic elements, especially when a small distortion happens.[5] So, linear incompatible 3D elements are chosen for the 3D discrete model, which is applied in Ls-Dyna.

Different from the 3D element, shell elements discrete a body by defining the geometry at a reference surface and transferring the initial 3D geometry to 2D. The membrane-shaped shell model is less stiff than the 3D element, and this helps the shell models encounter fewer convergence problems than the 3D element. Moreover, thanks to the reduction of model dimension, linear shell elements save more computational time than linear 3D elements with fewer nodes. Integration points are defined alone by the thickness of the shell model. However, shell elements regard those important parameters as the default property, which means that they do not calculate the thickness changing in the simulation. Therefore, such simplification may cause problems in proper contact, and this may result in inaccuracy.

Further comparation with the discrete 3D element model will be discussed in the Discussion session.

ISSN 2706-655X Vol.5, Issue 8: 42-48, DOI: 10.25236/IJFET.2023.050807

2. Nonlinear Finite Element Analysis

2.1 Model setup and property settings

The U-shape stamping process is simplified to a 1/4 model due to its geometry symmetry in X-direction and Z-direction. (Figure 1) Such simplification can not only reduce the memory cost but also cut down the computational time.

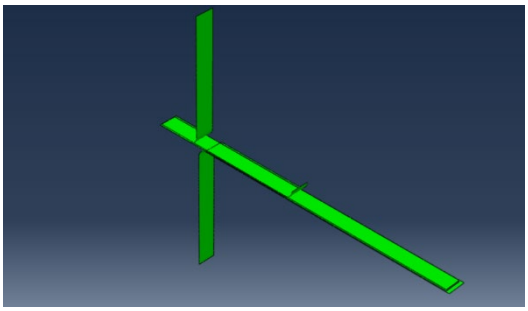

Figure 1: 1/4 model of U-shape bending.

2.2 Mesh Settings & Convergence Analysis

Three layers of elements are set through the thickness direction to increase the accuracy of the bending process. To further increase the accuracy of the simulation, Convergence analysis of the deformed stage is the next process to accomplish. Moreover, to increase the reliability of the convergence analysis, the blank mesh (Figure 2) is based on a specific mesh base. Finer mesh is applied at the circled region, where bending happens at the maximum punch stroke.

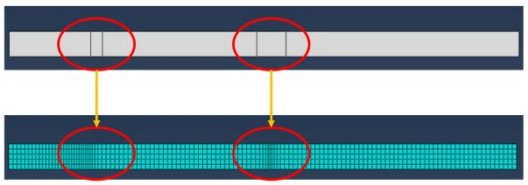

Figure 2: Divisional mesh for the blank.

The figure (Figure 3) below is the result of convergence analysis of the 3D models at the maximum punch stroke with distinct applied binder forces.

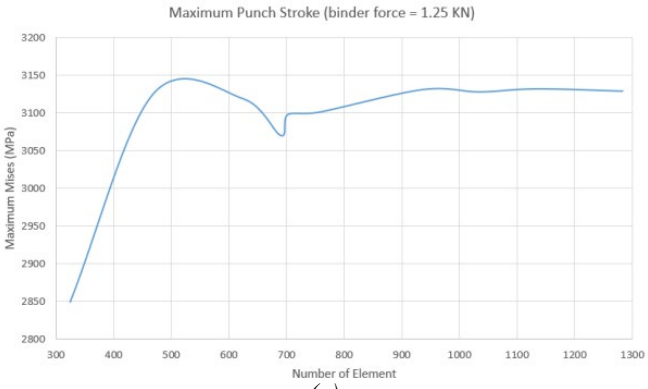

(a)

ISSN 2706-655X Vol.5, Issue 8: 42-48, DOI: 10.25236/IJFET.2023.050807

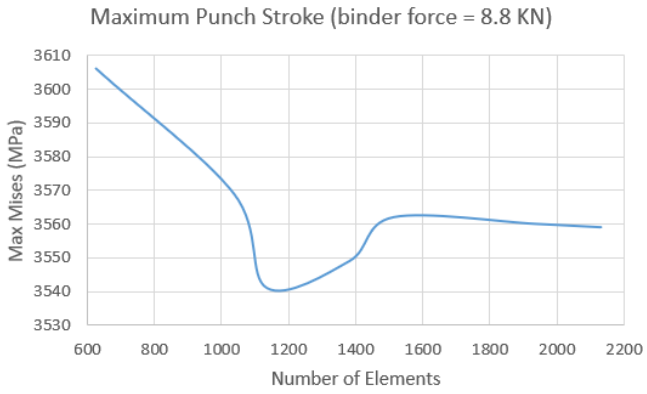

(b)

Figure 3: (a) Convergence analysis of the 3D models at the maximum punch stroke with binder force = 1.25 KN. (b) Convergence analysis of the 3D models at the maximum punch stroke with binder force = 8.8 KN.

3. Result & Discussion

3.1 Sensitivity to the binder force

Below are the contour plots of effective plastic strain and Von Mises stress of the 3D element constructed model (Figure 5).

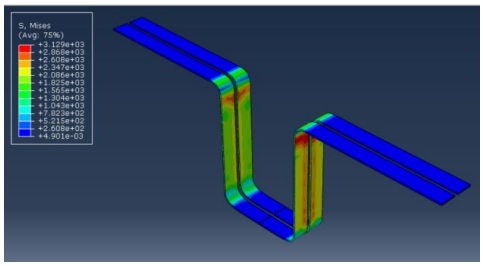

(a)

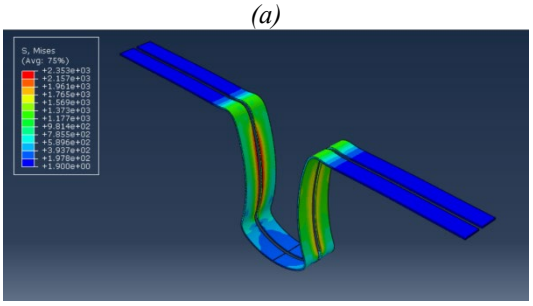

(b)

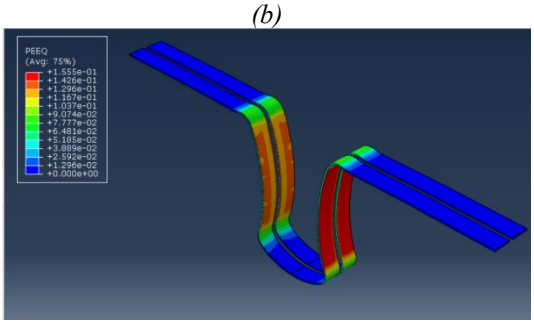

(c)

ISSN 2706-655X Vol.5, Issue 8: 42-48, DOI: 10.25236/IJFET.2023.050807

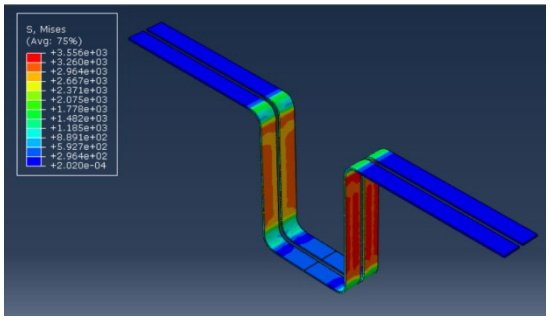

(d)

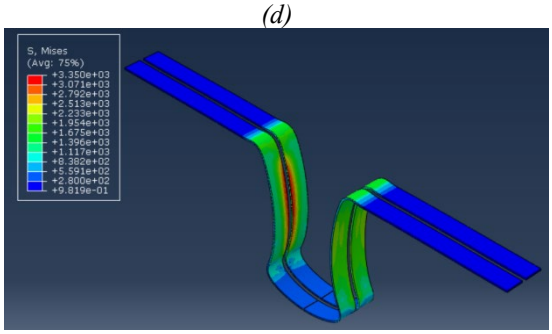

(e)

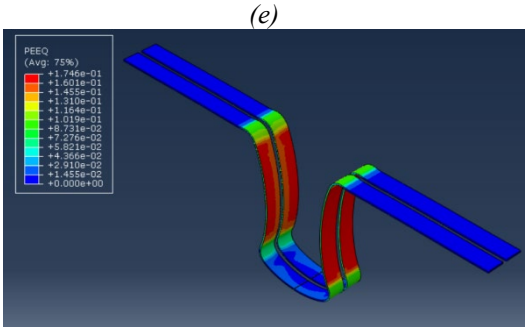

(f)

Figure 5: (a) Deformed shape plot at the maximum punch stroke (Binder force = 1.25KN). (b) Deformed shape plot after spring-back (Binder force = 1.25KN). (c): Contour plot of effective plastic strain (Binder force = 1.25KN). (d): Deformed shape plot at the maximum punch stroke (Binder force = 8.8KN). (e): Deformed shape plot after spring-back (Binder force = 8.8 KN). (f): Contour plot of effective plastic strain (Binder force = 8.8 KN).

A larger binder force will cause an increase in frictional force. Therefore, more external force applied to the punch is inevitable to deform the blank. As a result, a larger binder force will increase the norm of deviatoric stress, which is the von Mises stress, when bending the blank. The model withstood more force with the Binder Force, leaving more deviatoric strain after the force was removed.

Moreover, by comparing the thickness variation along the cord length of the blank (Figure 6), It is clear that the blank is thinner when a larger binder force is applied. The phenomenon could be explained that the punch induces mostly bending stresses in the material with low binder force. However, as the holder holds the blank more severely, the stresses induced by the punching phase become mostly tensile stresses. So, it is smooth to conclude that spring-back increases with decreasing binder force.

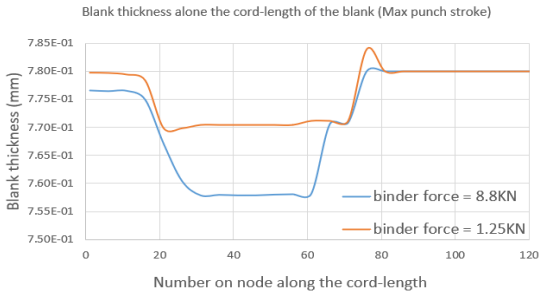

(a)

ISSN 2706-655X Vol.5, Issue 8: 42-48, DOI: 10.25236/IJFET.2023.050807

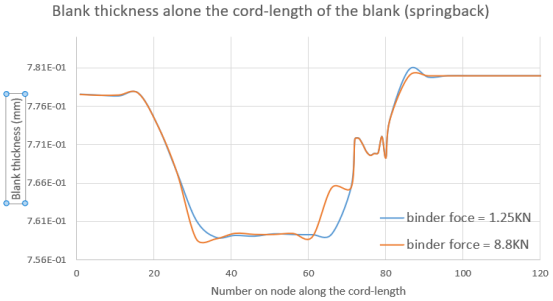

(b)

Figure 6: (a) Thickness variation along the cord length of the blank at the maximum punch stroke. (b) Thickness variation along the cord length of the blank after spring-back.

3.2 Comparison with the shell element

To compare shell and 3D element models, the planar mesh of shell models remains the same as that of 3D models, respectively. Below are the contour plots of effective plastic strain and von Mises stress of the shell element constructed model (Figure 7).

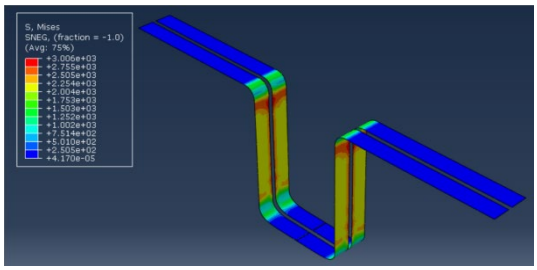

(a)

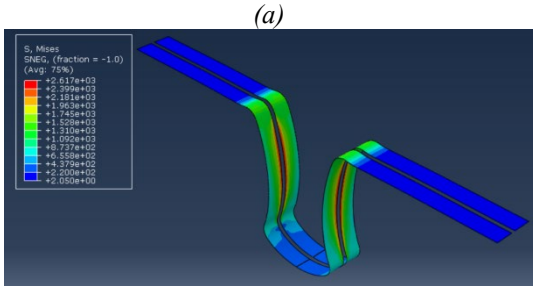

(b)

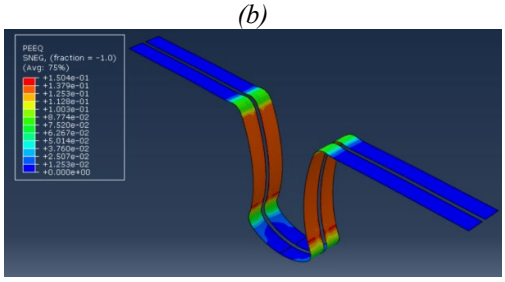

(c)

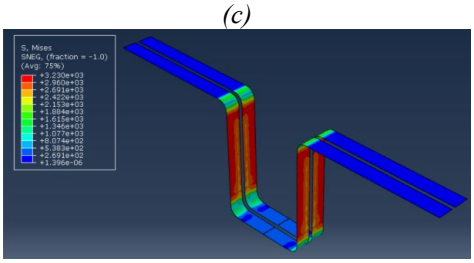

(d)

ISSN 2706-655X Vol.5, Issue 8: 42-48, DOI: 10.25236/IJFET.2023.050807

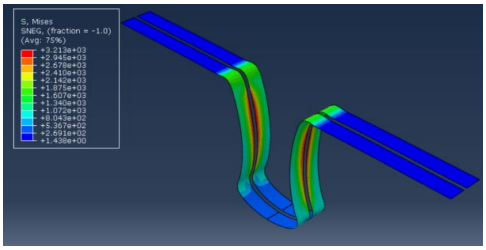

(e)

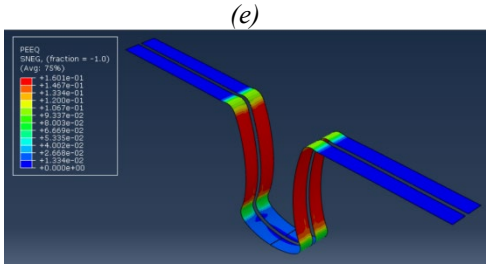

(f)

Figure 7 (a) Deformed shape plot at the maximum punch stroke (Binder force = 1.25KN). (b) Deformed shape plot after spring-back (Binder force = 1.25KN). (c): Contour plot of effective plastic strain (Binder force = 1.25KN). (d): Deformed shape plot at the maximum punch stroke (Binder force = 8.8KN). (e): Deformed shape plot after spring-back (Binder force = 8.8 KN). (f): Contour plot of effective plastic strain (Binder force = 8.8 KN).

By comparing with the 3D element constructed model, the shell element-based model could give similar Maximum Von-Mises stress and effective plastic strain.

To further compare the spring-back topology difference between the 3D element model and the shell element model, the sidewall curl and two bending angles (α_1 and α_2) are measured from the spring-back topology. Besides, the sidewall curl is measured based on the radius of a circle that passes the three points marked by three green circles on the sidewall. (Figure 8)

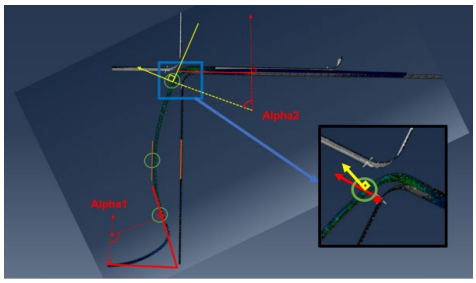

Figure 8: Description of the three quantities (α_1 and α_2) and side wall curl to quantify spring-back. r is the radius of the circle defined by three circled points.

Tables (Table 1&2) below illustrate the measured parameter of spring back model topology.

Table 1: Measured spring-back parameters from shell and 3D element model with 1.25KN binder force.

Model Description	α_1	α_2	side wall curl r (mm)
3D element	115.12	67.88	66.6401
Shell (5 layers)	114.42	68.13	76.3913
Shell (7 layers)	114.88	67.62	73.1382

Table 2: Measured spring-back parameters from shell and 3D element model with 8.8 KN binder force.

Model Description	α_1	α_2	Side wall curl r (mm)
3D element	111.51	69.89	80.1196
Shell (5 layers)	110.62	68.5	89.2817
Shell (7 layers)	110.52	66.64	85.4412

Based on the table above, though both shell and 3D elements predict a similar bending angle, the 3D

ISSN 2706-655X Vol.5, Issue 8: 42-48, DOI: 10.25236/IJFET.2023.050807

element model shows more spring back effect with a larger sidewall curl. Also, with more integration points along with the thickness, the shell element model has the trend to converge with the 3D model.

By comparing the spring-back topology and the maximum shell element model with different binder forces, the less spring-back effect appears with a larger binder force, which is similar to that of the 3D element. So, it is smooth to conclude that the shell element could give us reasonable results with the tolerance of some inaccuracy and less computational time.

4. Conclusion

In this research, a Finite Element Analysis in spring-back prediction with different element types and binder forces was described. The influence on spring-back of binder force and the performance of a shell and 3D elements is compared. Through the discussion, shell elements are recommended for U-shape bending.

References

[1] Chongthairungruang B, Uthaisangsuk V, Suranuntchai S, et al. Springback prediction in sheet metal forming of high strength steels [J]. Materials & Design, 2013, 50: 253-266.
[2] Wagoner R H, Lim H, Lee M G. Advanced issues in springback [J]. International Journal of Plasticity, 2013, 45: 3-20.
[3] Botelho T D S, Bayraktar E, Inglebert G. Comparison of experimental and simulation results of 2D-draw-bend springback [J]. Journal of Achievements in Materials and Manufacturing Engineering, 2006, 18(1-2).
[4] Kim N H. Introduction to nonlinear finite element analysis[M]. Springer Science & Business Media, 2014.
[5] Wilson E L, Ibrahimbegovic A. Use of incompatible displacement modes for the calculation of element stiffnesses or stresses[J]. Finite Elements in Analysis and Design, 1990, 7(3): 229-241.